

THE FORMATION AND GRAVITATIONAL-WAVE DETECTION OF MASSIVE STELLAR BLACK HOLE BINARIES

KRZYSZTOF BELCZYNSKI^{1,2}, ALESSANDRA BUONANNO³, MATTEO CANTIELLO⁴, CHRIS L. FRYER⁵,
DANIEL E. HOLZ^{6,7}, ILYA MANDEL⁸, M. COLEMAN MILLER⁹, AND MAREK WALCZAK¹

¹ Astronomical Observatory, Warsaw University, Al. Ujazdowskie 4, 00-478 Warsaw, Poland; kbelczyn@astrouw.edu.pl

² Center for Gravitational Wave Astronomy, University of Texas at Brownsville, Brownsville, TX 78520, USA

³ Maryland Center for Fundamental Physics and Joint Space-Science Institute, Department of Physics, University of Maryland, College Park, MD 20742, USA

⁴ Kavli Institute for Theoretical Physics, University of California, Kohn Hall, Santa Barbara, CA 93106, USA

⁵ Computational Computer Science Division, Los Alamos National Laboratory, Los Alamos, NM 87545, USA

⁶ Enrico Fermi Institute, Department of Physics, and Kavli Institute for Cosmological Physics, University of Chicago, Chicago, IL 60637, USA

⁷ Theoretical Division, Los Alamos National Laboratory, Los Alamos, NM 87545, USA

⁸ School of Physics and Astronomy, University of Birmingham, Edgbaston, Birmingham B15 2TT, UK

⁹ Department of Astronomy and Joint Space-Science Institute University of Maryland, College Park, MD 20742-2421, USA

Received 2014 April 8; accepted 2014 May 25; published 2014 June 20

ABSTRACT

If binaries consisting of two $\sim 100 M_{\odot}$ black holes exist, they would serve as extraordinarily powerful gravitational-wave sources, detectable to redshifts of $z \sim 2$ with the advanced LIGO/Virgo ground-based detectors. Large uncertainties about the evolution of massive stars preclude definitive rate predictions for mergers of these massive black holes. We show that rates as high as hundreds of detections per year, or as low as no detections whatsoever, are both possible. It was thought that the only way to produce these massive binaries was via dynamical interactions in dense stellar systems. This view has been challenged by the recent discovery of several $\gtrsim 150 M_{\odot}$ stars in the R136 region of the Large Magellanic Cloud. Current models predict that when stars of this mass leave the main sequence, their expansion is insufficient to allow common envelope evolution to efficiently reduce the orbital separation. The resulting black hole–black hole binary remains too wide to be able to coalesce within a Hubble time. If this assessment is correct, isolated very massive binaries do not evolve to be gravitational-wave sources. However, other formation channels exist. For example, the high multiplicity of massive stars, and their common formation in relatively dense stellar associations, opens up dynamical channels for massive black hole mergers (e.g., via Kozai cycles or repeated binary–single interactions). We identify key physical factors that shape the population of very massive black hole–black hole binaries. Advanced gravitational-wave detectors will provide important constraints on the formation and evolution of very massive stars.

Key words: binaries: general – black hole physics – gravitational waves – stars: early-type

Online-only material: color figures

1. INTRODUCTION

In the early universe massive ($M \gtrsim 100 M_{\odot}$) black holes (BHs) are believed to form from the collapse of massive stars (Fryer et al. 2001), and these BHs may be the seeds of the supermassive BHs at the nuclei of galaxies (Madau & Rees 2001; Whalen & Fryer 2012). These massive BHs have also been invoked to explain ultraluminous X-ray sources (so termed because they emit at 10–100 times the Eddington rate for a $10 M_{\odot}$ BH) in the nearby universe (Colbert & Mushotzky 1999; Miller & Colbert 2004). Until recently, both observations of stellar clusters, e.g., Figer (2005; although see also Massey 2003), and some theoretical arguments (McKee & Ostriker 2007) have suggested that stars above $150 M_{\odot}$ do not form at non-zero metallicities. Including the effects of mass loss from winds, even at one-tenth solar metallicity, this assumption produces masses of BH systems in the nearby universe in the tens of solar masses (Belczynski et al. 2010a).

However, the discovery of several stars with current masses greater than $150 M_{\odot}$ and initial masses up to $\sim 300 M_{\odot}$ in the R136 region of the Large Magellanic Cloud (Crowther et al. 2010) requires a rethinking of this argument. There are at least some environments in which stellar masses can apparently extend well beyond $150 M_{\odot}$, and if these stars do not have extremely large wind loss rates, then after their cores collapse they may leave behind BHs with masses in excess of $100 M_{\odot}$.

It has been suggested that stars with initial masses between roughly $150 M_{\odot}$ and $300 M_{\odot}$ at low to moderate metallicities explode due to an instability produced when the core gets so hot that it produces electron/positron pairs, resulting in a loss of energy which reduces the pressure and causes the core to contract. As this happens the nuclear burning accelerates and can disrupt the star entirely if the star is unable to stabilize itself. If some fraction of superluminous supernovae are in fact pair-instability supernovae (Woosley et al. 2007; Gal-Yam et al. 2009; Cooke et al. 2012; Ofek et al. 2014; see, however, Nicholl et al. 2013), then at least at metallicities around $\sim 0.1 Z_{\odot}$ (where $Z_{\odot} = 0.014$) massive stars above $150 M_{\odot}$ exist.

Gravitational waves (GWs) can potentially provide additional evidence for the formation and evolution of these massive stars. Massive stars are usually found in binaries or multiple systems (e.g., Kobulnicky & Fryer 2007; Kiminki & Kobulnicky 2012; Sana et al. 2012, 2013a) with mass ratios that are flat (Sana et al. 2013b). Indeed, the most massive known binary has an estimated total mass of 200–300 M_{\odot} and a possible initial mass of $\sim 400 M_{\odot}$ (Sana et al. 2013b). Thus massive BHs formed from the evolution of these massive stars are likely to be partnered with comparably massive BHs. If very massive stars (VMSs) with initial masses above $150 M_{\odot}$ also follow these trends, these stars may produce massive BH binaries, some of which may merge. Keeping the binary’s mass ratio fixed, the total energy emitted in GWs is proportional to the binary’s total

mass, so coalescing massive BH binaries can be detected much farther than stellar-mass BH binaries. Thus, they could be very significant sources for advanced GW detectors.

In this paper, we explore in detail the evolution of binaries with initial (zero-age main sequence, ZAMS) component masses above $150 M_{\odot}$ and the formation of very massive BH–BH binaries; the fate of binaries with initial component masses up to $150 M_{\odot}$ was explored elsewhere (Dominik et al. 2012). The formation of merging, massive BH binaries depends sensitively on a range of issues in stellar evolution—for example the evolution of the core, the expansion in the giant phase, and the details of the pair-instability supernovae. We discuss how these uncertainties lead to a wide range of predictions for the merger rates for these systems. Even an approximate measurement of the merger rates will place insightful constraints on these stellar processes. We discuss these uncertainties in detail, calculating the full range of rate predictions for advanced LIGO/Virgo.

In Section 2 we discuss the physical processes and uncertainties involved in the evolution of very massive binaries. In Section 3 we provide a range of predictions for the rates of formation and merger of massive binary stellar-mass BHs, based on different assumptions with different codes. In Section 4 we consider dynamical effects, particularly Kozai cycles and three-body interactions, and find that even if most or all massive BH binaries are too widely separated to merge on their own within a Hubble time, many will be induced to merge by interactions with other objects. In Section 5 we map these coalescence rate predictions for massive binaries to predictions for detection rates in future GW observatories. We emphasize the importance of the merger and ringdown phases of the gravitational waveform and cosmological effects, due to the high masses of the BHs and the significant redshift out to which they can be observed. Our discussion and conclusions are in Section 6.

2. BH–BH BINARY FORMATION PHYSICS

In this section we outline and discuss the basic evolutionary processes that are involved in the formation of close (with coalescence times below the Hubble time) BH–BH binaries from VMSs. Three major sources of uncertainty are involved.

1. *Common envelope evolution.* During this stage one of the stars in the binary expands such that its envelope surrounds both stars. In order to ultimately lead to a compact binary, the drag on the binary due to the envelope must shrink the semimajor axis, but must eject the envelope before the cores merge. There are many uncertainties about the efficiency with which this happens, as well as about the conditions necessary for common envelope evolution as opposed to stable mass transfer via Roche lobe overflow.
2. *Stellar radius expansion.* In order for the common envelope phase to be effective, it is necessary that the stars in the binary expand significantly when they go off the main sequence, because otherwise the stars would have had to be nearly in contact and would thus have likely merged due to tidal effects. However, current codes suggest the emergence of new effects for VMSs (such as convection that encompasses nearly the entire star) that may suppress such expansion. These effects appear to have complex dependencies on metallicity, rotation, and possibly even the code used to do the analysis.
3. *Black hole formation.* Massive stars (with initial mass $\lesssim 150 M_{\odot}$) form an iron core and undergo core collapse

at the end of their evolution, thereby forming BHs. VMSs ($\lesssim 300 M_{\odot}$) are potentially unstable to pair creation well before iron core formation. The subsequent pair-instability supernova may disrupt the entire star and thus prevent BH formation. For even more massive stars, pair creation cannot overcome the gravity of the collapsing star, and it is expected that the entire star will end up forming a BH. The transition from one regime to another depends on the internal temperature structure of a star and is very sensitive to assumptions in the stellar evolutionary codes. Additionally, there is significant uncertainty about the BH mass (whether it forms from a supernova explosion with its associated mass ejection, or whether the BH forms from the collapse of the entire star). Finally, it is possible that the resulting BH receives a significant natal kick, disrupting the binary and eliminating massive BH–BH systems.

We now discuss each of these issues in greater depth.

2.1. Common Envelope

The formation of a close binary of two BHs from the initially wide binary of two massive stars, which are large objects with ZAMS radii in excess of $10\text{--}30 R_{\odot}$ (e.g., Hurley et al. 2000), requires a process that leads to significant and fast orbital decay. In isolated evolution, where there is no dynamical interaction with other stars, a common envelope (CE) phase in which the expanding envelope of a post-main-sequence star engulfs the entire binary system is the only available process for sufficient orbital decay. For a recent comprehensive review of the physics of CEs and the many remaining uncertainties, see Ivanova et al. (2013).

To motivate this process in more detail, we recall that a star undergoes a series of burning phases, where the core contracts and heats up sufficiently such that the ashes of the previous phase are ignited and burn. Concurrent with these phases the envelope can also undergo phases of expansion. When the envelope reaches the companion, the friction of the companion orbiting in the envelope transfers orbital energy into the envelope. As a result, the envelope may eventually become unbound, leaving a binary system composed of the primary hot core and its mostly unaffected companion. A large orbital contraction (factors of $\gtrsim 10\text{--}100$) is expected for envelopes with mass $\gtrsim 10\%$ of the core mass ($\gtrsim 10\text{--}100 M_{\odot}$ for massive BHs). For binaries of two massive stars this process may occur twice, as first the primary and then the secondary undergo evolutionary expansion. This picture is generally accepted but, as we now describe, the details of the CE phase are both highly uncertain and extremely important for predicting the properties of any resulting stellar-mass BH binaries.

First, when the more massive star comes into contact with its Roche lobe, the binary is very likely eccentric and the individual stars are unlikely to have spins that are synchronized with the orbital motion because the evolution of massive stars is very rapid compared to the tidal timescale. Mass transfer therefore occurs during periastron passage. Whether such intermittent mass transfer continues, or whether it leads rapidly to circularization/synchronization is not known. This translates into a highly uncertain initial separation at the onset of the CE phase.

Second, it is not fully understood which binary configurations lead to a CE (i.e., mass transfer proceeding on a dynamical timescale) and which lead to stable Roche lobe overflow (RLOF; i.e., mass transfer proceeding on the donor’s nuclear or thermal timescale). A standard argument begins by noting that the

angular momentum of a circular binary with a semimajor axis a , total mass M , and reduced mass μ is $\mu\sqrt{GMa}$. In conservative mass transfer, $M = \text{const}$. Transfer from the more to the less massive star increases μ , whereas transfer from the less to the more massive star decreases μ . Angular momentum conservation thus implies that mass transfer from the more to the less massive object shrinks the binary. This is often used to argue that such transfer is unstable (compared to the stable mass transfer from the less to the more massive star).

The real situation is more complicated, particularly for very massive binaries. Mass and angular momentum can be lost from the system via winds, in some cases mass loss can shrink stars faster than the orbital separation shrinks, and it is in particular uncertain what happens for stars with radiative envelopes in large mass ratio binaries. Typically it is estimated that for mass ratios $q \lesssim 1/3$ – $1/2$ (where q is the ratio of the mass of the companion to the mass of the donor) and for donors with deep convective envelopes, RLOF will develop into CE. Both outcomes, CE and stable RLOF, are adopted in the literature (e.g., Hjellming & Webbink 1987; Tauris & Savonije 1999; Wellstein et al. 2001; Ivanova et al. 2003; Dewi & Pols 2003; Belczynski et al. 2008; Mennekens & Vanbeveren 2013).

Third, there is no self-consistent physical model to calculate reliably the post-CE orbital separation, which as we explained above is crucial to whether a system merges into one object or leads to a compact object binary, and whether such a binary can merge within the age of the universe. There are two existing approaches. One uses an energy balance prescription which unfortunately does not conserve the angular momentum of the system (Webbink 1984). The other uses an angular momentum balance prescription which unfortunately does not conserve energy (Nelemans & Tout 2005). The two methods may differ by as much as an order of magnitude in their predictions for post-CE orbital separation. Each method has had success in reproducing the orbital periods of separate groups of post-CE white dwarf binaries. It is not known which method (if either) is a reasonable approximation for very massive binaries with BHs.

Fourth, the donor envelope binding energy directly affects the fate of the binary after the CE phase, because as we describe above the envelope must be ejected to leave the core. If the binding energy is too large, the components will merge. If the binary survives, the final separation depends on the value of the binding energy. There is, however, ambiguity in the definition of the envelope binding energy because it is difficult to precisely define the core-envelope boundary. Different choices in the literature (e.g., Tauris & Dewi 2001; Podsiadlowski et al. 2003; Voss & Tauris 2003; Xu & Li 2010; Loveridge et al. 2011) include a specific level of H-depletion, an entropy jump, or the position of the H-burning shell. Given that most of the mass and binding energy of the envelope are from the part of the envelope near the core, these choices may influence common envelope calculations. It has been suggested that double compact object merger rates may be affected by as much as an order of magnitude (T. M. Tauris 2012, private communication), while recently it was argued that the specific choice for the core-envelope boundary does not play a significant role for massive stars (i.e., black hole progenitors with $M_{\text{zams}} \approx 70$ – $100 M_{\odot}$; Wong et al. 2013). If the internal energy of the envelope is significant, this could make ejection easier. Similarly, if there are nuclear burning shells in the envelope they could affect the ejection process, although the sign of this effect is unclear. Finally, even for a given envelope binding energy the ejection process will be affected by the fraction of the dissipated orbital

energy which goes into the ionization and dissociation of atoms and molecules in the envelope rather than into bulk kinetic energy.

Fifth, for many massive stars the most significant radial expansion occurs right after the main sequence, as the rapid core adjustment after the end of core hydrogen burning causes the star to rapidly cross the Hertzsprung gap (HG). Hence it is expected that many massive binaries will initiate the CE phase during the HG. However, it is not clear whether at this point the stars already have a well developed core-envelope structure. Some models indicate that the entropy profile is rather flat throughout the HG (i.e., it has similar structure to a main sequence star), which means that once the CE begins it will always end in a merger of both components. Other models suggest that if the core of the donor is exposed during this evolutionary phase (i.e., by the inspiraling companion), it may remain at its compact size and thus there is the potential for CE survival.

2.2. Stellar Radius Evolution

For a common envelope to develop, the radius of at least one of the stars must increase more rapidly than the Roche lobe radius. Because the Roche lobe radius is $R_{\text{RL}} \sim (m/M)^{1/3}a$, where m is the mass of the donor, M is the mass of the binary, and a is the binary separation, this requirement is approximately equivalent to the requirement that the fractional expansion of the radius of one of the stars must exceed the fractional increase in the binary separation. VMSs at non-zero metallicity (e.g., Population I stars with heavy element fractions $Z = 0.002$, such as those in the Small Magellanic Cloud) may lose half or more of their mass to stellar winds during the main sequence (e.g., Yusof et al. 2013). If mass is removed from a circular binary without changing the specific angular momentum \sqrt{GMa} , the binary's separation would double when half of the mass is lost. Thus the binary separation can increase by a factor of ~ 2 on the main sequence, and therefore to initiate a CE phase one of the binary components needs to expand by more than a factor of 2.

However, as indicated above, if there is a CE phase during the main sequence then the shallow entropy gradient leads to full inspiral and merger. Survival of the CE phase requires that it be initiated beyond the main sequence, when the core-envelope structure is well-developed and thus the envelope can be ejected while the core is unaffected. The radius evolution of a VMS is therefore critical to the fate of very massive binaries, but this evolution is currently uncertain because it depends, rather sensitively, on the treatment of convection, stellar winds, and rotational mixing in stellar models.

For example, models of $500 M_{\odot}$ stars done with the Geneva code (Yusof et al. 2013) show no radial expansion beyond the main sequence for metallicities $Z = 0.014$ (solar) and $Z = 0.006$, and only a mild expansion for $Z = 0.002$ (from $\sim 50 R_{\odot}$ at the middle of the main sequence to $\sim 110 R_{\odot}$ after hydrogen core exhaustion). Given that, as indicated above, the orbit can expand by up to $\sim 30\%$ during this time, it is difficult for a binary to enter the CE phase and thus to produce a close massive BH–BH binary.

This expected behavior is qualitatively distinct from that of stars below $\sim 100 M_{\odot}$, which are believed to expand significantly after the main sequence. The difference for VMSs is that they are thought to have large convective cores (up to 90% of the stellar mass at the ZAMS for a star with an initial mass of $200 M_{\odot}$, and up to 95% of the stellar mass for a star with an initial mass of $500 M_{\odot}$; see Yusof et al. 2013). These cores stem

from the large radiation pressure at such high masses, and mean that fresh hydrogen is constantly being brought to the center and helium is mixed to the photosphere. In the models this leads to strong Wolf–Rayet (WR) winds that can remove almost all of the hydrogen from the envelope, resulting in highly helium-rich stars that experience little expansion.

The treatment of mixing induced by convection and rotation, along with the adopted wind mass loss rates, are the crucial factors in modeling the radial expansion of VMSs. However both prescriptions are quite uncertain. Typical treatments are mostly based on theoretical estimates that are only weakly constrained by observations (especially in the case of rare VMSs). Therefore, large uncertainties exist in the resulting radius evolution, leading to outcomes anywhere between two extremes: (1) no/small radial expansion, no/small envelope mass after the main sequence (Yusof et al. 2013), (2) significant radial expansion, large envelope mass after the main sequence. Latter results were obtained using MESA calculations of VMSs, where a decisive effect in the radial extension of the radiation-dominated regions of VMSs is envelope inflation (see, e.g., Kato 1985; Ishii et al. 1999; Petrovic et al. 2006; Gräfenor et al. 2012).

In stellar evolution calculations crude approximations are made in order to deal with the energy transport in these complex layers which largely affect the final radii of the stars (Paxton et al. 2013). For example, in the outer layers of the envelope the temperature decreases to few $\times 10^5$ K and iron recombines, leading to a large opacity (see, e.g., Cantiello et al. 2009). As a result, in these layers the stellar luminosity is much larger than the Eddington luminosity, which might seem to imply that convection will dominate energy transport. However, due to the very low density in the envelope, convection is very inefficient (superadiabatic) and cannot transport all of the energy, leaving some of it “trapped” in the envelope. A possible (but not unique) solution is that these layers expand, which changes the opacity profile and allows the trapped energy to escape. This leads to an inflation of the stellar radius and the formation of a density inversion (e.g., Petrovic et al. 2006; Gräfenor et al. 2012). We note that in some codes this inflation does not occur because, for numerical reasons, convection is assumed to be able to transport the entire energy flux (see, e.g., Maeder 1987; Paxton et al. 2013). This effect is shown in Figure 1 where the photospheric radius evolution during the main sequence of a $500 M_{\odot}$ at $Z = 0.002$ is calculated using two different assumptions for the efficiency of convective energy transport. These models have been calculated using MESA with the usual mixing length theory (MLT) or assuming an enhancement of the convective energy transport (MLT++, see Section 7.2 in Paxton et al. 2013). These models are non-rotating and assume the mass loss recipe of Glebbeek et al. (2009). The result shown by the solid line is in good agreement with a similar calculation using the GENEVA code (Yusof et al. 2013).

It is estimated (Petrovic et al. 2006; Gräfenor et al. 2012) that the mass contained in the shells that would be affected by this inflation is rather small: $10^{-9} M_{\odot}$ for WR stars and $10^{-2} M_{\odot}$ for luminous blue variable stars. However, the inflation can extend the radius of a star by a factor of a few. This in turn may lead to the onset of a CE phase for very massive binaries on relatively close orbits. Once the CE phase is initiated we require a significant envelope mass (in excess of $10 M_{\odot}$) to efficiently decrease the orbital separation and form a close BH–BH system. For example, if we start with a massive binary ($400 M_{\odot} + 200 M_{\odot}$) in an orbit with $a = 340 R_{\odot}$, the orbital separation will decrease to 290, 120, 14 R_{\odot} for envelope masses

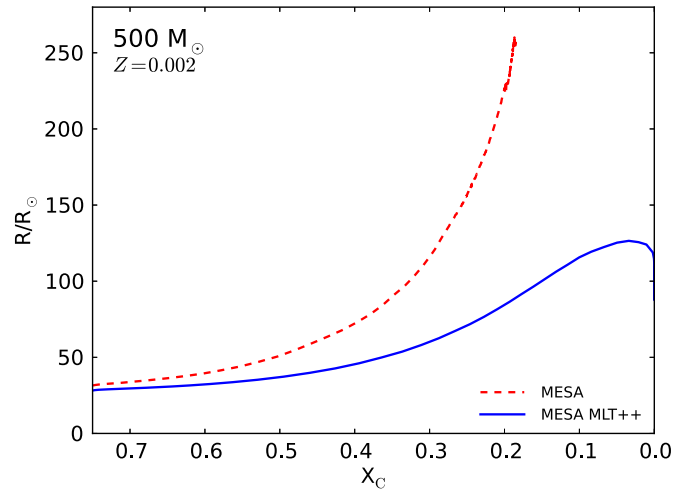


Figure 1. Evolution of the photospheric radius as function of hydrogen core mass fraction (X_C) for MESA calculations of a $500 M_{\odot}$ model at $Z = 0.002$. The dashed line shows a model where the convective energy transport is calculated according to the mixing length theory (MLT). The radial expansion is substantial and is associated with a density inversion in the stellar envelope. In this situation very short timesteps pose problems for the code and the model could not be evolved past $X_C \simeq 0.18$. The solid line shows the same calculation assuming an enhancement in the efficiency of convective energy transport (MLT++). In this case no envelope inflation occurs and the code can evolve the star to the end of the main sequence.

(A color version of this figure is available in the online journal.)

of 1, 10, $100 M_{\odot}$, respectively. Here we have applied the most effective orbital contraction (by assuming energy balance) with fully efficient transfer of orbital energy to the envelope ($\alpha_{CE} = 1.0$) and with large envelope binding energy ($\lambda = 0.1$).

Therefore it appears that VMSs at low metallicity may or may not have massive H-rich envelopes (due to the uncertainties in the treatment of internal mixing and wind mass loss rates) and that these envelopes may or may not expand significantly after the main sequence (due to the uncertainties in the modeling of radiation-dominated stellar envelopes). To assess the influence of these uncertainties on our predictions we consider two extremes in Section 3. For the first we employ evolutionary models for VMSs that show both significant expansion and large envelope mass beyond the main sequence. For the second we assume that VMSs do not expand at all and therefore have no interactions in isolated (e.g., field stellar populations) binary evolution.

2.3. Black Hole Formation

For stars above $100 M_{\odot}$, the mass of the star at the point of core collapse generally determines the remnant mass. If the carbon/oxygen (CO) core mass is above $\sim 7.6 M_{\odot}$ (see, e.g., Section 2.3 of Belczynski et al. 2010a), it is likely that the core will collapse to a BH without producing a supernova explosion, so the mass of the compact remnant is simply the mass of the star at collapse. However, if the core has sufficient angular momentum, a disk can form around the newly formed BH with the potential to produce a gamma-ray burst (Woosley 1993; MacFadyen & Woosley 1999). In a series of $250 M_{\odot}$ star simulations, assuming efficient internal angular momentum transport from magnetic torques, Woosley & Heger (2012) found that even without mass loss (and the resulting angular momentum loss), only the outer layers (containing $\sim 16 M_{\odot}$) of these stars have sufficient angular momentum to produce a disk and drive an outflow. Any such outflow will have a small effect

(<5–10%) on the final BH mass. Overall our uncertainty about the mass loss from stellar winds dominates the uncertainties in mass estimates of the star at collapse and therefore of its compact remnant.

VMSs can produce massive helium cores (above $45 M_{\odot}$) that, after helium burning, can undergo an instability where pair-production reduces the pressure in the core, allowing it to collapse. Compressional heating in the collapse causes the CO and Si cores to reach much higher temperatures than occurs in normal core burning, and the resulting burning phase can be so explosive that, in the most extreme cases, there is no remnant. These are the hypothesized pair-instability supernova (Barkat et al. 1967; Bond et al. 1984; Carr et al. 1984; Glatzel et al. 1985; Fryer et al. 2001; Chatzopoulos et al. 2013). For a sufficiently massive core, the center of the star is so hot that the photodisintegration instability is encountered before explosive burning reverses the shock, accelerating the collapse (Bond et al. 1984; Fryer et al. 2001). These stars collapse to form large BHs and the mass at which this photodisintegration instability prevents explosions marks the upper limit on the pair-instability progenitor mass. Whether or not the pair instability can disrupt a star depends upon the conditions in the core, in particular the helium core mass, which as discussed above depends on the details of stellar mixing. The lower and upper initial star mass limits for pair-instability supernovae are typically thought to be roughly $150 M_{\odot}$ and $300 M_{\odot}$ (Fryer et al. 2001), respectively, but these limits are sensitive to the aforementioned uncertainties on the size of the helium core. To avoid confusion with the initial mass range dependence on metallicity, the above limits are typically translated to final CO core masses of 60, $130 M_{\odot}$ (e.g., Yusof et al. 2013) for the pair-instability mechanism to operate.

Natal kicks during supernovae are another source of uncertainty in this modeling. It may happen that during core collapse a natal kick will modify the orbit in such a way as to increase the eccentricity and/or decrease the orbital separation. Potentially, a close double BH binary may form. However, it is very unlikely that such a favorable kick is encountered, so only a very small fraction of binaries may be affected by this process. Nonetheless, such effects could lead to the formation of massive BH–BH binaries in some cases. The tremendous reach of advanced ground-based instruments means that such coalescences need only happen a few percent of the time to lead to many detections per year.

Supernova natal kicks may play an additional role in these massive stars. Without supernova explosions, kick mechanisms relying on asymmetric mass ejecta (e.g., Herant et al. 1992; Buras et al. 2003; Blondin et al. 2003) will not work. In the absence of kicks, we expect the spin axes to be aligned for the resulting binary BH systems. This is because binary stars (1) may have been formed with rotation aligned with the orbital axis (although see Albrecht et al. 2014 for examples of non-aligned binaries), (2) may have been subject to strong tidal interactions if on relatively close orbits (although see Claret 2007 for a discussion of very inefficient radiative damping and tidal torquing for massive stars) and (3) mass transfer and/or common envelope episodes may have aligned component rotation with the orbital angular momentum for close interacting binaries (although see Sepinsky et al. 2010 for examples when mass transfer does not necessarily lead to effective tidal torquing and circularization/synchronization). If this is the case, then the alignment of spin axes could be used to distinguish a binary origin of massive BH–BH mergers from a dynamical

origin. However, mechanisms invoking asymmetries in the neutrino emission (e.g., Kusenko & Segrè 1996, 1997; Socrates et al. 2005; Fryer & Kusenko 2006) are able to drive kicks as long as electron neutrinos are trapped in the collapsed core. These mechanisms require large magnetic fields ($\gtrsim 10^{15}$ G). For massive stars with ZAMS masses above $1000 M_{\odot}$, the electron neutrino trapping region is small, but below this mass (which encompasses all the systems of interest in this paper), the trapping region can be large (Fryer & Heger 2011). It is therefore possible that a neutrino driven kick mechanism may work. Such kicks would alter our population studies and produce non-aligned spin axes and would reduce close BH–BH formation rates. Without a better quantitative understanding of these kicks, however, it is difficult to assess their effects.

3. ESTIMATES OF BH–BH MERGER/FORMATION RATES

In this section we give the results from two models that give a reasonable span of possible rates. In Model 1 we assume that VMSs expand significantly and have massive H-rich envelopes beyond the main sequence. In this approach we use population synthesis to estimate the merger rates of massive close BH–BH binaries. In Model 2 we assume that VMSs do not expand significantly beyond the main sequence and we use simple order-of-magnitude estimates to assess the formation rates of wide massive BH–BH binaries. In both models we use an energy balance approach for the CE phase. We also limit the range of pair-instability supernovae to stars that form final CO core masses of 60– $130 M_{\odot}$ and assume that in this range no BHs are formed. Outside this range we assume that the entire star collapses to form a BH (minus the 10% of the mass that we assume leaves in the form of neutrino emission). Therefore, we neglect any potential mass loss from collapsar outbursts. We also assume that these massive stars do not impart natal kicks during the formation of their BHs. In Section 4 we will explore dynamical processes to show that these may shorten the merger time of these wide BH–BH binaries below a Hubble time and make them potentially important for advanced GW detectors.

3.1. Model 1: Expanding VMS

3.1.1. Initial Conditions

Recent evidence suggests that VMSs exist above 1%–10% solar metallicity (where $Z_{\odot} = 0.014$), but little is known yet about their initial conditions in binaries, e.g., their initial mass function, binary fractions, and orbital separations. We assume that the stellar initial mass function for the primary mass $M_{\text{zams},a}$ has the form $dN/dM \propto M^{-\alpha}$ with $\alpha = 1.3$ for the range $0.08 M_{\odot}$ – $0.5 M_{\odot}$, $\alpha = 2.35$ for $0.5 M_{\odot}$ – $1 M_{\odot}$, and $\alpha = 2.7$ for $M > 1 M_{\odot}$ (Kroupa et al. 1993; Weidner et al. 2011). We only consider here VMSs with $150 M_{\odot} < M_{\text{zams},a} < 1000 M_{\odot}$. We also assume a companion mass $M_{\text{zams},b} \leq M_{\text{zams},a}$ drawn from a distribution uniform between 0 and 1 in the mass ratio $q \equiv M_{\text{zams},b}/M_{\text{zams},a}$ (e.g., Sana et al. 2012), a uniform-in-the-log distribution of orbital separations and a thermal-equilibrium distribution of eccentricities ($P(e) = 2e$ in range $e = 0$ – 1 ; Heggie 1975; Duquennoy & Mayor 1991). If VMSs expanded as much as $M_{\text{zams}} < 150 M_{\odot}$ stars, these distributions would ensure that $\sim 50\%$ of binaries would experience Roche lobe overflow during their lifetime, leading to a potential common envelope and subsequent orbital contraction (Sana et al. 2013a); however, the lack of significant expansion of VMSs may limit such interactions. We only evolve binaries for which $M_{\text{zams},b} > 150 M_{\odot}$

as in this study we are focused on VMS evolution and the formation of massive BH–BH binaries. We assume a binary fraction of 50% (i.e., 2/3 of stars are in binaries). We also assume that 50% of the stars in the local universe (within the reach of advanced GW instruments) have solar metallicity and 50% of the local stars have $Z = 0.002$ ($\sim 10\% Z_{\odot}$).

Some of these assumptions have linear effects on the predicted rate. For example, changing the number of massive stars by a factor of two will change the number of mergers by a factor of two, and changing the close binary fraction by a factor of two changes the number of mergers by roughly a factor of two. In contrast, our uncertainties about stellar evolution and binary interactions have nonlinear effects, and will dominate the errors in our rate estimates for the foreseeable future.

3.1.2. Population Synthesis Calculations

Binary evolution calculations are treated as described in full detail by Belczynski et al. (2008) with several recent updates on stellar wind mass loss rates, compact object mass distribution and CE handling as outlined by Dominik et al. (2012). In particular, we employ wind mass loss rates from Vink et al. (2001). We use energy balance for CE evolution that employs fully efficient transfer of orbital energy into the CE (i.e., $\alpha = 1$) with physical calibration of donor binding energy (Xu & Li 2010). A criterion for the development of CE is based on donor expansion/contraction in response to mass loss and the related response of donor Roche lobe due to mass transfer and orbital angular momentum losses. This approximately translates into CE development for binaries with donors significantly (factor of $\gtrsim 2$) more massive than their companions or with donors with deep convective envelopes (e.g., red giants). We apply the rapid supernova explosion model, which reproduces the mass gap between neutron stars and BHs, to obtain compact remnant masses (Belczynski et al. 2012).

The community currently lacks fully accepted models of VMSs at high metallicity. In lieu of such models, we extend the stellar evolutionary formulae of Hurley et al. (2000) to calculate the evolution and fate of stars up to a ZAMS mass of $M_{\text{zams}} = 1000 M_{\odot}$ using the population synthesis code StarTrack (Belczynski et al. 2008). We apply a direct extrapolation with no high-mass specific modifications to the original Hurley et al. (2000) models. We combine these formulae with the wind mass loss rates compiled and calibrated by Belczynski et al. (2010a). This scheme was originally developed for stars with $M_{\text{zams}} \lesssim 100\text{--}150 M_{\odot}$. These extrapolated VMS models expand significantly and form massive H-rich envelopes beyond the main sequence, as expected for stars with $M_{\text{zams}} \lesssim 100\text{--}150 M_{\odot}$.

In our solar metallicity models the CO core mass is approximately $12 M_{\odot}$ for a broad range of initial stellar masses, $M_{\text{zams}} = 100\text{--}500 M_{\odot}$ (Figure 2). At higher ZAMS masses the CO core mass rises sharply to a maximum of $\sim 280 M_{\odot}$ for $M_{\text{zams}} = 800 M_{\odot}$, then decreases for higher initial star masses. At subsolar metallicity, the CO core mass is roughly $40 M_{\odot}$ for $M_{\text{zams}} = 100\text{--}300 M_{\odot}$, above which the core mass rises monotonically to a maximum of $300 M_{\odot}$ for $M_{\text{zams}} = 1,000 M_{\odot}$. As we indicated in Section 2, the BH mass approximately traces the CO core mass, and so depends on the initial stellar mass in the same way that the CO core mass does, for both solar and subsolar metallicity. However, whereas the maximum CO core mass is roughly the same for solar and subsolar models, the maximum BH mass is much greater for subsolar metallicity stars. This is because at subsolar metallicity the highest mass

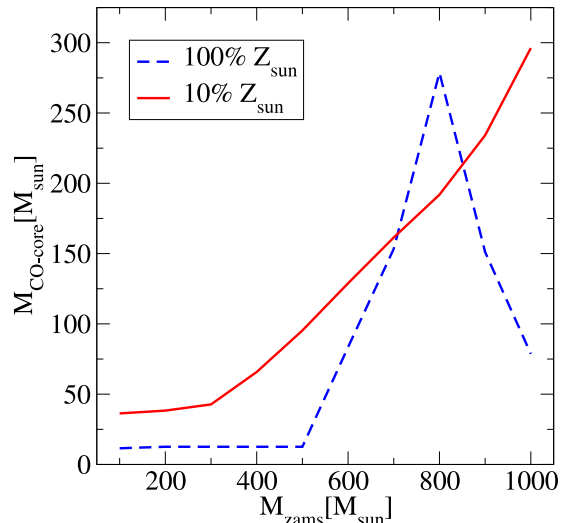


Figure 2. Final CO core mass (just prior to core collapse and BH formation) for our evolutionary models of very massive stars. Here the stars are assumed to be either single or non-interacting binary components, so this figure is only illustrative and is not directly relevant for binary evolution leading to the formation of close BH–BH systems.

(A color version of this figure is available in the online journal.)

stars retain their H-rich envelope, whereas at solar metallicity winds can efficiently remove the entire envelope.

Our calculation of CO core mass is based on the combination of extrapolated stellar models presented by Hurley et al. (2000) and the wind mass loss rates collected and calibrated by Belczynski et al. (2010a). Within this framework the initial flatness of the dependence of CO core mass on ZAMS mass is the result of increasing strength of wind mass loss with ZAMS mass. Stars below $M_{\text{zams}} = 500 M_{\odot}$ and $M_{\text{zams}} = 300 M_{\odot}$ for solar and subsolar metallicity, respectively, are stripped of their H-rich envelopes and they become WR stars. This further increases mass loss. Low metallicity stars above $M_{\text{zams}} = 300 M_{\odot}$ have such massive H-rich envelopes that they never become WR stars, and their pre-supernova mass (and therefore CO core mass) increases monotonically with ZAMS mass. This happens also for solar metallicity stars above $M_{\text{zams}} = 500 M_{\odot}$. However, at some point, high metallicity stars are subject to wind mass loss strong enough to remove even very massive H-rich envelope and they become massive WR stars. Strong WR-type wind mass loss leads to the efficient decrease of star mass. For stars above $M_{\text{zams}} = 800 M_{\odot}$ the final CO core mass decreases with initial ZAMS mass.

These results may be compared to the detailed stellar evolutionary models of massive stars published by Yusof et al. (2012). They found that at solar metallicity the final CO cores have masses $15\text{--}20 M_{\odot}$ (assuming no rotation) or around $25\text{--}35 M_{\odot}$ (with significant rotation), for $M_{\text{zams}} = 100\text{--}500 M_{\odot}$. Our relation for the same regime is also flat but results in lower CO core masses ($12 M_{\odot}$). Their lowest metallicity model, which has a metallicity of $\sim 10\%$ solar ($Z = 0.002$; appropriate for the Small Magellanic Cloud), shows a monotonic increase of final CO core mass from $90 M_{\odot}$ to $140 M_{\odot}$ in the mass range $M_{\text{zams}} = 150\text{--}300 M_{\odot}$. Our relation is flatter in that regime and results in lower CO core masses ($40\text{--}50 M_{\odot}$). In both solar and subsolar metallicity evolution our evolutionary models result in lower CO core masses than are predicted by Yusof et al. (2012). Therefore, our estimate of BH mass is conservatively low compared with the published detailed evolutionary models

Table 1
Very Massive Star Model Properties^a

Phase	Mass M_{\odot}	Radius R_{\odot}	M_{CO} M_{\odot}	Comment
Start MS	500	50	...	$Z = 0.014$
End MS	48	5	...	
End He-burning	26	1	20	BH formation
Start MS	500	50	...	$Z = 0.006$
Mid MS		100	...	
End MS	102	7	...	
End He-burning	75	2	65	Pair inst. SN
Start MS	500	30	...	$Z = 0.002$
Mid MS		50	...	
End MS		10	...	
Post MS		100	...	
End He-burning		<65	150	BH formation

Note. ^a These results are taken (or extrapolated) from the rotating Yusof et al. (2013) models.

(see Figure 2). We also stress that for the relatively high metallicities, $Z > 0.4 Z_{\odot}$, considered by Yusof et al. (2012), winds drive away the entire H-rich envelope for high-mass stars. This is consistent with our findings, but may not be true for lower metallicity stars.

We can also compare our results to the additional models in Yusof et al. (2013). Here we will focus on the highest mass models in these calculations, with an initial mass of $M_{\text{zams}} = 500 M_{\odot}$; somewhat lower-mass stars (e.g., $M_{\text{zams}} = 300 M_{\odot}$) evolve in qualitatively similar ways. We will use only their rotating models, as these are more physical than non-rotating models. Table 1 shows the results from the calculations in Yusof et al. (2013). For the solar-metallicity $500 M_{\odot}$ star, the mass of the star is $26 M_{\odot}$ at the end of core helium burning, dropping to $20 M_{\odot}$ when the CO core forms. Such a star will most likely collapse to a BH with mass similar to the mass of its CO core mass. At about 40% solar metallicity ($Z = 0.006$; typical of the Large Magellanic Cloud), the mass of the star at the end of the main sequence is $102 M_{\odot}$ and at the end of core helium burning is $75 M_{\odot}$. The star forms a $65 M_{\odot}$ CO core and at this mass it is likely to undergo a pair instability supernova that completely disrupts the star and does not leave behind a compact object remnant. For 10% of solar metallicity, extrapolating the results from Yusof et al. (2013) suggests that a $M_{\text{zams}} = 500 M_{\odot}$ star ultimately produces a CO core mass of $150\text{--}170 M_{\odot}$. The most likely fate of such a star is core collapse and the formation of a BH with a mass of about $150 M_{\odot}$. For comparison, a $300 M_{\odot}$ model at this metallicity finishes the main sequence as a $176 M_{\odot}$ star, and ends core helium burning as a $150 M_{\odot}$ star that forms a CO core with a mass of $135 M_{\odot}$. This CO core will likely form a BH of similar mass.

3.1.3. Population Synthesis Results

We find that only low metallicity environments/host galaxies could contribute significantly to the formation of close BH–BH systems from VMSs. This is qualitatively the same result as obtained for lower mass stars (Belczynski et al. 2010b). Most of the close very massive BH–BH systems (75%) merge with short delay times ($t_{\text{delay}} < 1$ Gyr).

For subsolar metallicity there are two separate populations of BH–BH systems. Most of the systems (93%) form with total mass $M_{\text{tot}} = 50\text{--}100 M_{\odot}$ and average mass ratio of $q = 0.9$, while there is a smaller population (7%) of BH–BH systems

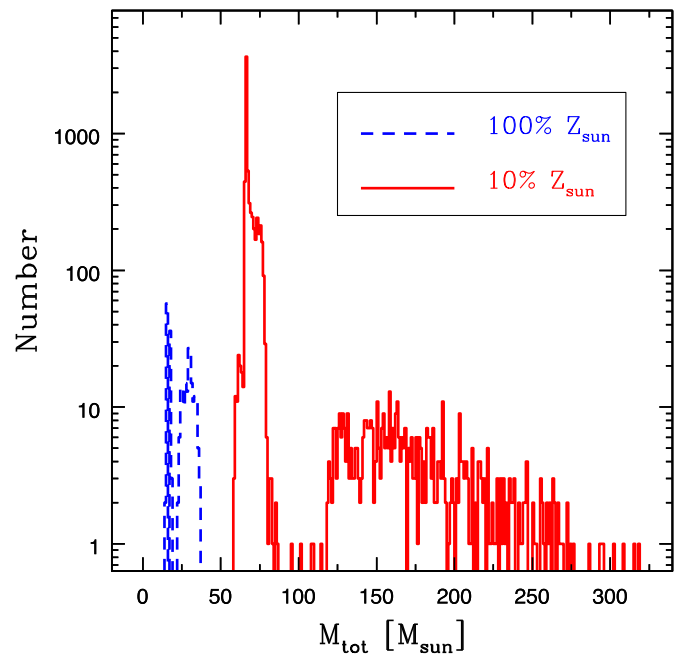


Figure 3. Total mass of close (merging within a Hubble time) BH–BH binaries produced in our Model 1 with population synthesis calculations. Note that the low metallicity environment dominates BH–BH formation. Also note two distinctive BH–BH subpopulations at low metallicity: one with $M_{\text{tot}} < 100 M_{\odot}$ and one with $M_{\text{tot}} > 100 M_{\odot}$.

(A color version of this figure is available in the online journal.)

with $M_{\text{tot}} = 100\text{--}300 M_{\odot}$ and average mass ratio of $q = 0.8$ for subsolar metallicity. The less massive systems originate from stars with $M_{\text{zams}} \approx 150\text{--}500 M_{\odot}$, whereas the more massive ones evolve from stars with $M_{\text{zams}} \approx 500\text{--}1000 M_{\odot}$. For solar metallicity, there are virtually no BH–BH systems with total mass $M_{\text{tot}} > 40 M_{\odot}$.

We consider only close BH–BH binaries with total mass $M_{\text{tot}} > 100 M_{\odot}$, as these binaries provide a clear signature of VMS existence and evolution. The lower mass systems may have originated from regular stars (i.e., $M_{\text{zams}} < 150 M_{\odot}$). These massive BH–BH systems would have aligned spins (as no supernova explosion and hence no natal kick is expected for such massive stars; Fryer et al. 2012). If core collapse for such massive stars leads to a stalled shock rather than mass loss in a supernova, the BHs that are formed will include the entire angular momentum of the pre-collapse progenitor. This is likely to lead to rapidly spinning BHs. Our major results discussed above are presented in Figure 3–5.

With all of the previously discussed uncertainties, it is very difficult to produce reliable quantitative results for BH binaries. However, within the framework of these extrapolated normal stellar models we find that the common envelope phase is almost always initiated by a star when it expands immediately after the main sequence, i.e., during HG evolution. If we assume the binary can survive this common envelope phase and that pair instability supernovae do not occur for Population I stars ($Z > 0.1 Z_{\odot}$, which encompasses all our models), we find that BH–BH merger rates are $0.5 \times 10^{-6} \text{ yr}^{-1}$ per Milky Way equivalent galaxy (MWEG) for BH–BH systems with total masses larger than $100 M_{\odot}$. This corresponds to a merger rate density of $5 \times 10^{-9} \text{ yr}^{-1} \text{ Mpc}^{-3}$. This is our most optimistic estimate. If we allow for pair instability supernovae as discussed in Section 2 then the rates drop by two orders of magnitude and we find that the BH–BH merger rate density is

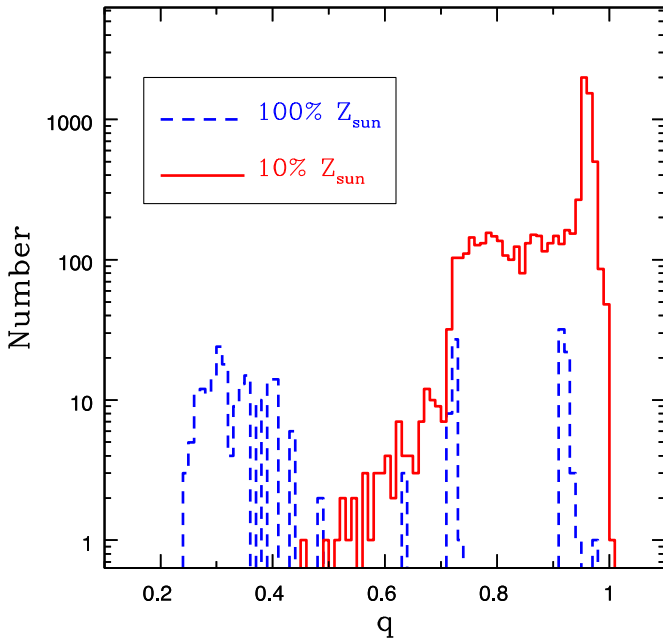


Figure 4. Close BH–BH binary mass ratio (less massive to more massive) for our Model 1. Note that mass ratios are rather high and are typically in range $q = 0.7$ – 1 for the dominant low metallicity BH–BH population.

(A color version of this figure is available in the online journal.)

$5 \times 10^{-11} \text{ yr}^{-1} \text{ Mpc}^{-3}$. This is probably our most realistic model. If we increase our CO core masses by a factor of two (consistent with Yusof et al. (2013), who find CO cores ~ 1.5 – 3 times more massive than ours), the rate increases to $3 \times 10^{-9} \text{ yr}^{-1} \text{ Mpc}^{-3}$. This is because our CO core masses for close BH–BH systems with $M_{\text{tot}} > 100 M_{\odot}$ are $M_{\text{CO}} = 50$ – $100 M_{\odot}$, which is in the pair instability supernova range $M_{\text{CO,pair}} = 60$ – $130 M_{\odot}$. Doubling our CO core masses therefore moves most of them above the pair instability range and thus allows many additional systems to evolve to BH–BH binaries. Finally, if we do not allow for CE survival with HG donors the merger rates drop to zero.

We note that all of our findings in this section are a direct result of our *assumption* that VMSs of high metallicity behave qualitatively like normal massive stars. If they do, then the large volume in which massive BH coalescence could be seen with advanced LIGO/Virgo suggests that the observed rate could be many per year. The observation of even one of these systems would refute the arguments against radial expansion of VMSs (Yusof et al. 2013), and would show that these binaries can survive the CE phase with HG donors. These constraints would provide insight into stellar evolution models. If the rate is high, we could even place limits on the formation conditions of these massive binaries (e.g., the binary mass ratio and initial mass function).

3.2. Model 2: Non-expanding VMS

In this model we assume that there is no significant expansion of VMSs. This means that both binary components evolve as single stars, and in the end either form BHs or are disrupted by pair-instability SNe. The initial orbital separation only expands due to the wind mass loss. There is no CE phase that could decrease orbital separation as both binary components are within their respective Roche lobes. Since we assume no natal kicks at the formation of the BHs, all binaries with components that are not subject to pair-instability SNe should form wide BH–BH binaries (i.e., with merger times much longer than the Hubble

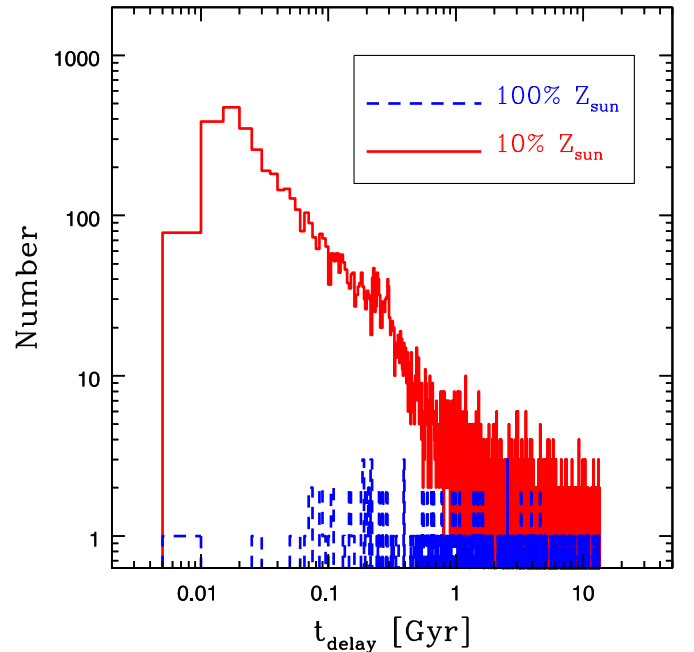


Figure 5. Delay time distribution of close BH–BH binaries for our Model 1. Note that the distribution for the dominant low metallicity BH–BH population falls off approximately as t_{delay}^{-1} . The delay time is defined as time elapsed from star formation (ZAMS) to the final BH–BH coalescence.

(A color version of this figure is available in the online journal.)

time). However, as we discuss in Section 4, dynamical processes may be able to tighten such binaries so that they do merge within a Hubble time. Here we present an order-of-magnitude estimate of the formation rate of these wide BH–BH systems. We will limit our estimate only to systems with BHs of $100 M_{\odot}$ or more¹⁰.

We make the same assumptions about the initial mass function as before, extending it to an upper limit of $10^3 M_{\odot}$. The wind-driven mass loss rate for high-mass stars is extremely uncertain, as is the dependence of this rate on metallicity. It is therefore unclear what initial mass is required to leave behind a $100 M_{\odot}$ BH, but for an order-of-magnitude estimate we will assume that $M_{\text{zams}} > 500 M_{\odot}$ is sufficient to form a $100 M_{\odot}$ BH. For comparison, our extrapolated evolutionary models produce a $100 M_{\odot}$ BH for $M_{\text{zams}} > 600 M_{\odot}$ and $M_{\text{zams}} > 400 M_{\odot}$ for solar and 10% solar metallicity, respectively. For the initial mass function we have assumed, we find a fraction $\approx 2 \times 10^{-6}$ of stars will start with masses above $500 M_{\odot}$. If, as we assumed previously, the binary mass ratio distribution is roughly flat, then \sim half of the stars will have companions at least half as massive as they are, and thus binary evolution will presumably produce comparable-mass BHs.

Let us suppose that only some fraction of these binaries can avoid pair-instability supernova. Following our earlier discussion we assume that stars with final CO core mass above $130 M_{\odot}$ avoid this fate and form massive BHs. Extrapolation of results presented by Yusof et al. (2012; see their Figure 18) suggests that only stars at subsolar metallicity can avoid pair instability SNe and form massive BHs above $100 M_{\odot}$. It appears that at $Z = 0.002$ (SMC) all stars with $M_{\text{zams}} > 500 M_{\odot}$ form these massive BHs, whereas only a small fraction (if any) of

¹⁰ Note that in Model 1 we have only considered BH–BH binaries with total mass above $100 M_{\odot}$, while the Model 1 total mass distribution extended to about $300 M_{\odot}$.

stars with $M_{\text{zams}} > 500 M_{\odot}$ form massive BHs for $Z = 0.006$ (such as for the Large Magellanic Cloud). At higher metallicities (e.g., for the Milky Way) no massive BHs are expected. Given that the metallicity distribution of stars is poorly constrained, we assume that only 10^{-1} can avoid pair-instability SNe for $M_{\text{zams}} > 500 M_{\odot}$.

The Galaxy has $\sim 2 \times 10^{11}$ stars, so our collection of assumptions implies that $\sim 2 \times 10^4$ wide very massive BH binaries per Milky Way Equivalent Galaxy (MWEG) will be produced by a stellar binary population. The Galaxy is $\sim 10^{10}$ years old, and the comoving number density of MWEGs is $\sim 10^{-2} \text{ Mpc}^{-3}$ (e.g., Kopparapu et al. 2008). Thus the formation rate density, averaged over cosmic history, is $\sim 10^{-8} \text{ Mpc}^{-3} \text{ yr}^{-1}$. In Section 5 we discuss how these rates translate into advanced LIGO detection rates.

We can similarly estimate the formation rate of $\gtrsim 100 M_{\odot}$ BHs with $\sim 10 M_{\odot}$ BH companions. These intermediate-mass-ratio binaries are of significant interest as their inspirals may serve as precise probes of the spacetime around BHs (Amaro-Seoane et al. 2007; Brown et al. 2007; Gair et al. 2011; Rodriguez et al. 2012). If we continue to assume that the mass ratio distribution is flat, then we would expect $\sim 10 M_{\odot}$ BHs to be companions to $> 100 M_{\odot}$ BHs in $\sim 10\%$ of systems, leading to a formation rate of $\sim 10^{-9} \text{ Mpc}^{-3} \text{ yr}^{-1}$.

4. DYNAMICAL PROCESSES AFFECTING MASSIVE BINARIES

As we have discussed, current stellar evolutionary theory suggests that although massive main sequence binaries have a good chance of evolving into massive BH binaries, those binaries seem unlikely to be close enough that, on their own, they will coalesce within a Hubble time. However, many or most massive stars are born in stellar associations with initial number densities of hundreds of stars or more per cubic parsec. Hence after the formation of a double BH system there are additional interactions that can harden the binary. In addition, there is evidence that massive stars are, in a few to $> 10\%$ of cases, in triple or higher-order systems (e.g., Kiminki et al. 2012; Kiminki & Kobulnicky 2012; Duchêne & Kraus 2013). Such systems can potentially undergo Kozai resonance cycles (Kozai 1962; Lidov 1962) that increase the eccentricity of the massive binary sufficiently so that orbital energy and angular momentum loss through the emission of GWs could cause rapid coalescence. In this section we examine these effects and show that a significant fraction of initially wide very massive binaries may merge within a Hubble time, and possibly much sooner.

4.1. Binary–Single Interactions

Suppose that our massive binary is born into a cluster with a central mass density of $\rho \equiv 10^3 \rho_3 M_{\odot} \text{ pc}^{-3}$; note that R136 has a central density of at least $1.5 \times 10^4 M_{\odot} \text{ pc}^{-3}$ (Selman & Melnick 2013), and that other young clusters such as the Arches cluster can be even denser (Lang et al. 2001). If our massive binary has a total mass M and a semimajor axis a , and if we assume that the single objects that encounter the binary have much lower mass and need to get to within a distance $\sim a$ of the center of mass of the binary to affect the binary semimajor axis and eccentricity, then for a relative speed v_{∞} at infinity the cross section for the interaction is

$$\Sigma = \pi a^2 \left(\frac{2GM}{av_{\infty}^2} + 1 \right). \quad (1)$$

Stellar associations typically have velocity dispersions of a few km s^{-1} , so the first term in the parentheses dominates as long as a is less than $\sim 10^3 \text{ AU}$. For the same reason, interactions of interloping stars with the binary will tend to harden the binary and change its eccentricity e , causing it to sample a “thermal” distribution $P(e)de = 2ede$ (see Heggie 1975 for a pioneering study). Interaction with interlopers with a total mass approximately $2\pi/22$ times the binary’s mass will reduce the semimajor axis by a factor of ~ 3 (Quinlan 1996). The time needed to interact with this much mass is

$$T = \frac{M}{\rho \Sigma v_{\infty}} \approx 6 \times 10^8 \text{ yr } \rho_3^{-1} \left(\frac{a}{10 \text{ AU}} \right)^{-1} \left(\frac{v_{\infty}}{3 \text{ km s}^{-1}} \right). \quad (2)$$

Note that because $\Sigma \propto v_{\infty}^{-2}$, a smaller velocity dispersion implies a more rapid hardening of the binary. Note also that M does not appear, because the greater number of interactions required is offset by the larger gravitationally focused cross section. If the interloping objects are sufficiently massive then significant kicks could be delivered to the binary in the binary–single interactions, but if the binary is much more massive than typical stars (which we assume to be the case) then the binary should be able to remain within the stellar cluster. We also note that because massive objects tend to swap into binaries, initially solitary massive BHs have a good chance to become members of binaries in a short time (again, see Heggie 1975 for an early discussion of this process).

If the binary orbit were forced to remain circular, then its GW inspiral time is (Peters 1964)

$$T_{\text{GW}}(e = 0) = 5a^4 c^5 / (256G^3 \eta M^3) \\ \approx 1.6 \times 10^{15} \text{ yr} \left(\frac{\eta}{0.25} \right)^{-1} \left(\frac{M}{200 M_{\odot}} \right)^{-3} \left(\frac{a}{10 \text{ AU}} \right)^4, \quad (3)$$

where $\eta = m_1 m_2 / M^2$ is the symmetric mass ratio for objects of masses m_1 and m_2 and total mass M ; we have normalized η to 0.25, which is its maximum value and which occurs for equal masses. For a binary of eccentricity e that is reasonably near unity, this time becomes (Peters 1964)

$$T_{\text{GW}}(e \approx 1) \approx (768/425)(1 - e^2)^{7/2} T_{\text{GW}}(e = 0). \quad (4)$$

Thus for a binary of two $100 M_{\odot}$ BHs in a 1 AU orbit, an eccentricity of ≈ 0.895 (0.88 if the full expression from Peters 1964 is used rather than the approximation (4)) is enough to drop the merger time to 1 Gyr. If the BH binary has $a = 10 \text{ AU}$, the needed eccentricity for a 1 Gyr merger time is ≈ 0.992 .

Binary–single interactions will thus drive up the eccentricity until the inspiral time becomes short and the binary will merge (see Gültekin et al. 2006 and Mandel et al. 2008 for similar arguments in the case of massive BH binaries and intermediate-mass-ratio inspirals, respectively, in globular clusters). As discussed above, the eccentricity distribution ($P(e) = 2e$) is sampled roughly uniformly in each interaction in the limit of three objects of comparable mass. In the limit of a massive binary and very low-mass interlopers, Quinlan (1996) showed that three-body interactions increase the eccentricity of the binary steadily but slowly. For example, from Quinlan’s formulae, a $100 M_{\odot}$ – $100 M_{\odot}$ binary with $a = 10 \text{ AU}$ in a cluster of velocity dispersion $\sigma = 3 \text{ km s}^{-1}$ will increase its eccentricity from 0.7 to 0.99 in the time needed to reduce a by 2.4 e -foldings ($\sim 1 \text{ Gyr}$ for our parameters), and from 0.7 to 0.999 in the time needed to reduce a by 3.4 e -foldings. Eccentricity fluctuations

due to finite-mass interlopers will likely decrease the time to a given eccentricity. The details depend on the initial distribution of semimajor axes and eccentricities, and on the mass density of the cluster and the cluster's longevity, but it is plausible that in a significant fraction of cases where massive BH binaries form from stellar evolution, they are induced to merge by repeated dynamical encounters. The tilting of orbits during the dynamical encounters means that the BH spins will typically not be aligned with the orbit during merger.

4.2. Triple Systems and the Kozai Mechanism

Another way that initially widely separated massive BH binaries might coalesce involves triple systems. Observed massive stars have a probability, possibly greater than 10%, of being in triple or higher-order systems (e.g., Kiminki et al. 2012; Kiminki & Kobulnicky 2012; Duchêne & Kraus 2013). If the relative inclination of the inner binary and the tertiary is in the appropriate range, then over many orbits of both the binary and the tertiary the mutual inclination will oscillate between two limits in such a way that the eccentricity also oscillates (Kozai 1962; Lidov 1962; Lidov & Ziglin 1976). In the standard Kozai approximation, in which the tertiary has a fixed and effectively infinite angular momentum, the maximum eccentricity reached during a cycle is $(1 - (5/3) \cos^2 i)^{1/2}$, where i is the initial relative inclination. For example, if $i = 70^\circ$, the maximum eccentricity is 0.9. If, as is likely in our case, the binary has as much or more angular momentum as the tertiary, then the critical mutual inclination deviates from 90° (see, e.g., Lidov & Ziglin 1976; Miller & Hamilton 2002), so the probability of achieving a high eccentricity assuming random inclinations will be somewhat smaller than it would be for a critical inclination of 90° .

The time for a single Kozai cycle (from minimum to maximum eccentricity and back) is of order $\sim(M/m)(b/a)^3$ times the orbital time of the binary, where M is the mass of the binary, m is the mass of the tertiary, b is the semiminor axis of the tertiary, and a is the semimajor axis of the binary (e.g., Lidov & Ziglin 1976). For $a = 10$ AU, $b/a = 10$, $M = 200 M_\odot$, and $M/m = 100$ (reasonable fiducial values), this time is roughly 2×10^5 yr, which is much less than the time between close interactions with interloping stars. Thus systems that are favorably inclined for the Kozai resonance can complete many cycles without being harassed by interlopers.

General relativistic pericenter precession can limit the maximum eccentricity during a Kozai cycle. However, from the expressions in Miller & Hamilton (2002), this is not a limiting factor in our case. From their Equation (6), the maximum eccentricity that can be attained for a binary of two $100 M_\odot$ BHs at 1 AU orbited by a $10 M_\odot$ object with a semiminor axis of 10 AU is 0.99, far above the $e \approx 0.9$ needed for merger within 1 Gyr. If the binary has a semimajor axis of 10 AU and the tertiary has a semiminor axis of 100 AU, the maximum eccentricity is 0.9999, compared with the $e \approx 0.99$ for a 1 Gyr merger. Note that such an eccentricity can be achieved by $\sim 10\%$ of systems for an isotropic distribution of initial mutual inclinations.

Thus, depending on the fraction of triple systems and the distribution of the masses, inclinations, and separations of the tertiaries, it is possible that a few percent of initially wide VMS binaries (tens of percent of the $\sim 10\%$ of systems that are triples) are induced to merge by Kozai cycles. Such mergers would not have spins aligned with their orbits, because orbital tilting is produced during the cycles. The studies of Blaes et al. (2002) suggest that merger will happen near the point of minimum mutual inclination between the tertiary and binary, and if this is

at a point where the more massive BH in the binary is reasonably aligned with the orbital axis and the binary component mass ratio is not more than $\sim 2 : 1$, additional effects during the inspiral could help to align the axes further (Schnittman 2004).

In summary, in addition to the possibility of merger through isolated binary evolution (which remains viable because of uncertainties in massive binary evolution), there are at least two dynamical scenarios that might produce mergers of a few percent or more of the massive BH binaries that are too wide to merge in a Hubble time through radiation reaction alone. Coalescences through isolated binary evolution are likely to yield binary BHs with nearly aligned spins whose magnitude is close to the astrophysical maximum, if supernova kicks for these binaries are minimal. Coalescences involving dynamical processes will probably produce unaligned mergers, but because the BHs will have formed before the dynamical interactions the spins may still be close to maximal. Thus detections will probe a variety of stellar evolutionary and dynamical processes. We now discuss how coalescences between such objects could be detected.

5. DETECTION OF BH–BH COALESCENCES

Advanced LIGO (Harry & the LIGO Scientific Collaboration 2010) and Virgo (Virgo Collaboration 2009) interferometric GW detectors are coming online within a few years, and are expected to reach design sensitivity by the end of the decade (LIGO Scientific Collaboration et al. 2013). In addition to improving overall sensitivity by a factor of ~ 10 relative to their initial versions (Abbott et al. 2009; Accadia et al. 2012), these detectors will also extend the sensitivity to lower frequencies, down to ~ 10 Hz, which will allow GW signatures of massive BH binary mergers to be detected (see Abadie et al. 2012 for upper limits from searches with initial LIGO and Virgo detectors). Matched filtering against known templates describing expected signals is the optimal technique for extracting weak GW signals from noisy data. Although a network of multiple detectors is needed to rule out noise artifacts and separate signals from background, a good rule of thumb for detectability, which we follow here, is to consider a single detector and impose a matched-filtering signal-to-noise ratio (S/N) threshold of 8 as a proxy for detectability by the network (Abadie et al. 2010).

The detection rate R_d can be expressed in terms of the merger rate per unit comoving volume per unit time \mathcal{R} as an integral over all possible merger redshifts

$$R_d = \int_0^\infty \mathcal{R}(z) \frac{dV_c}{dz} \frac{dt_s}{dt_o}(z) f_d(z) dz. \quad (5)$$

Here the comoving volume of a given redshift slice dV_c/dz is computed (e.g., see Hogg 1999) by assuming WMAP9 parameters $\Omega_M = 0.282$, $\Omega_\Lambda = 0.718$, $h = 0.697$ (Hinshaw et al. 2013). The factor $dt_s/dt_o = 1/(1+z)$ is the ratio between the clock at the source redshift z , which measures the merger rate, and a clock at the Earth, which measures the detection rate. The detection fraction $f_d(z)$ measures the fraction of sources of a given mass at a given redshift that will be detectable.

The expectation value of the optimal matched filtering S/N for an overhead, face-on source is given by

$$S/N_{\text{opt}}^2 = 4\Re \int_0^\infty \frac{|\tilde{h}(f)|^2}{S_n(f)} df, \quad (6)$$

where $S_n(f)$ is the noise power spectral density of the detector and $\tilde{h}(f)$ is the frequency-domain representation of a

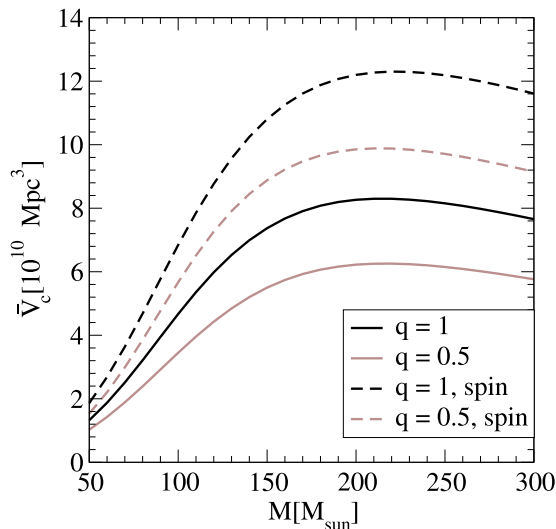


Figure 6. Detection-weighted sensitive comoving volume \bar{V}_c within which a coalescence could be detected for BH binaries with total source-frame mass M , mass ratios $q = 1$ or 0.5 , either non-spinning or with dimensionless spins magnitudes 0.6 .

(A color version of this figure is available in the online journal.)

GW signal. For the waveforms $h(t)$, we use spinning, non-precessing, inspiral-merger-ringdown effective-one-body waveforms calibrated to numerical relativity waveforms (Taracchini et al. 2012), specifically their *SEOBNRv1* implementation in the LIGO Scientific Collaboration Algorithm Library (LIGO Scientific Collaboration & Virgo Collaboration 2013). The waveform is corrected for the redshift z and its amplitude is inversely proportional to the luminosity distance to the source, which scales with z according to the assumed standard cosmology (Hogg 1999). Face-on, overhead equal-mass binaries with a total rest-frame mass of $200 M_\odot$ can be detected to a redshift of $z \sim 2$ (luminosity distance of ~ 16 Gpc) if the components are non-spinning, or $z \sim 2.6$ (luminosity distance of ~ 21 Gpc) if both components have aligned spins with a dimensionless magnitude of 0.6 .

The actual S/N for a binary with a given sky location α, δ , inclination ι , and polarization ψ is given by $S/N_{\text{opt}} \times \Theta(\alpha, \delta, \iota, \psi)/4$, where the projection function Θ is defined in Finn (1996). We compute the fraction $f_d(z)$ by taking into account the (numerically computed) cumulative distribution function (CDF) of $\Theta/4$, and setting the detectability threshold at an S/N of 8 as follows (e.g., Belczynski et al. 2013):

$$f_d(z) = 1 - \text{CDF}_{\Theta/4} \left[\min \left(\frac{8}{S/N_{\text{opt}}(z)}, 1 \right) \right]. \quad (7)$$

Under the simplifying assumption that the merger rate \mathcal{R} is constant in redshift, which we use here, Equation (5) for the detection rate can be written as

$$R_d = \mathcal{R} \bar{V}_c, \quad (8)$$

where we have defined the detection-weighted sensitive comoving volume \bar{V}_c for a given rest-frame mass combination as

$$\bar{V}_c = \int_0^\infty \frac{dV_c}{dz} f_d(z) \frac{1}{1+z} dz. \quad (9)$$

In Figure 6 we plot the detection-weighted comoving volume as a function of the total system mass in the source frame

for mass ratios $q = 0.5$ and $q = 1$, and spins that are either zero or both aligned with the angular momentum, with dimensionless magnitude 0.6 . We use the noise spectral density of the high-power, zero-detuning configuration (LIGO Scientific Collaboration & Virgo Collaboration 2011), which corresponds to nominal sensitivity that is expected for advanced LIGO detectors by the end of the decade (LIGO Scientific Collaboration et al. 2013). As expected, we find that when the mass ratio is equal and the aligned spins are high, signals contain more power and the sensitive volume is increased.

Equation (8) and Figure 6 allow us to convert a merger rate into a detection rate. In Section 3.1.3 we obtained a most optimistic merger rate of $5 \times 10^{-9} \text{Mpc}^{-3} \text{yr}^{-1}$ for BH–BH mergers with total mass above $100 M_\odot$. The peak of the total mass distribution for this model appears at $200 M_\odot$ and the BHs are of comparable mass. The weighted detectable volume for $M_{\text{tot}} = 200 M_\odot$ is $6\text{--}12 \times 10^{10} \text{Mpc}^3$ depending on BH spins, which yields 300–600 detections per year. Our more realistic estimate, which accounts for pair-instability SNe, produces a merger rate estimate of very massive BH–BH binaries of $5 \times 10^{-11} \text{Mpc}^{-3} \text{yr}^{-1}$, with a predicted detection rate of 3–6 a year. If we account for potential uncertainties in CE evolution the merger rate decreases to zero, and no detections are predicted for very massive BH–BH binaries in the isolated evolutionary scenario (Model 1).

In Section 3.2 we argued for a plausible order-of-magnitude formation rate of $\sim 10^{-8} \text{Mpc}^{-3} \text{yr}^{-1}$ for wide binaries with $100 M_\odot$ or more massive BHs. In Section 4 we estimated that $\sim 10\%$ of these wide binaries may merge within a Hubble time due to dynamical interactions with other stars. This yields a merger rate of $\sim 10^{-9} \text{Mpc}^{-3} \text{yr}^{-1}$ and a corresponding detection rate of ~ 100 per year if dynamical interactions are efficient in forming close very massive BH–BH binaries (Model 2).

We also considered intermediate-mass-ratio binaries of $\gtrsim 100 M_\odot$ BHs with $\sim 10 M_\odot$ BH companions, and concluded that a formation rate of $\sim 10^{-9} \text{Mpc}^{-3} \text{yr}^{-1}$ was plausible from order-of-magnitude arguments. Assuming that such systems can be brought to merge within a Hubble time by efficient dynamical hardening of the binary (e.g., Mandel et al. 2008), they can be detected to $z \sim 0.5$, which decreases the sensitive volume by a factor of ~ 20 relative to the $100 M_\odot\text{--}100 M_\odot$ case discussed above. Therefore, up to ~ 5 intermediate-mass-ratio systems formed from VMSs with lower-mass companions could be detected per year with advanced GW instruments.

It is also interesting to compare the population synthesis model predictions with existing upper limits from initial LIGO and Virgo runs. Their sensitivity to massive BH binaries was poor because of the high value of the low-frequency cutoff, so the more interesting existing LIGO/Virgo constraint will come from BH binaries with total mass between 50 and 100 solar masses. As reported in Section 3.1.3, such binaries represent 93% of our entire close BH–BH population, and this corresponds to a merger rate of $7 \times 10^{-8} \text{Mpc}^{-3} \text{yr}^{-1}$ for our most optimistic prediction. These binaries have formed from stars with initial mass $M_{\text{zams}} \approx 150\text{--}500 M_\odot$. The initial LIGO/Virgo upper limits are $1.7 \times 10^{-7} \text{Mpc}^{-3} \text{yr}^{-1}$ and $0.9 \times 10^{-7} \text{Mpc}^{-3} \text{yr}^{-1}$ for equal mass BH binaries in the mass bins $M_{\text{tot}} = 54\text{--}73 M_\odot$ and $M_{\text{tot}} = 73\text{--}91 M_\odot$, respectively (Aasi et al. 2013b). Thus even our most optimistic rates do not violate the current upper limits for BH–BH detection.

Given our predictions of preferentially aligned spins for isolated binaries and the possibility of spins misaligned with the orbital angular momentum for systems in which dynamics

played an important role, it is interesting to ask how well such systems can be distinguished based on GW observations. Several studies that considered a few individual events suggest that at least the spin magnitude of the more massive component and the angle between it and the orbital angular momentum could be measured, especially if this component is rapidly spinning, although it may prove difficult to measure the spin of the lower-mass secondary (e.g., van der Sluys et al. 2008; Raymond et al. 2010). A larger study (Vitale et al. 2014) supports this view, and highlights the improvements to spin measurement when the binary is nearly edge-on rather than face-on, and when the angular momentum of the secondary is small, reducing spin-spin terms. Furthermore, Bayesian model selection may allow us to determine whether there’s significant support for precession induced by spin-orbit misalignment even if individual parameters cannot be measured precisely (e.g., Aasi et al. 2013a). Unfortunately, the large size of the parameter space makes difficult a fully systematic study based on astrophysically motivated source distributions.

We conclude this section by pointing out the importance of (1) accurate analytical and numerical modeling of inspiral-merger-ringdown waveforms, since for massive BH–BH binaries, the S/N accumulates mostly during the last stages of the binary evolution (e.g., see Hinder et al. 2013), and (2) low-frequency detector sensitivity in searches for massive BH binaries, which contribute most of the S/N below ~ 35 Hz. The sensitive volume plotted in Figure 6 assumes that the predicted high-power, zero-detuning sensitivity (LIGO Scientific Collaboration & Virgo Collaboration 2011) will be achieved down to 10 Hz, which will require significant commissioning effort. Meanwhile, third-generation ground-based detectors such as the Einstein Telescope (Punturo et al. 2010), with sensitivity down to a few Hz, will be able to probe such massive BH–BH binaries to $z \sim 15$ (e.g., Gair et al. 2011).

6. DISCUSSION AND CONCLUSIONS

Since GWs from massive BH binaries can be detected to cosmological distances, we have explored the event rates for the mergers of these systems. We find that only low-metallicity environments ($Z \lesssim 0.1\text{--}0.4 Z_{\odot}$) may be favorable for the formation of very massive stellar-origin BHs with mass exceeding $100 M_{\odot}$. The formation of such BHs is possible if (1) the initial mass function (IMF) extends above $500 M_{\odot}$, (2) pair-instability SNe do not disrupt all stars above $500 M_{\odot}$, and (3) stellar winds for such massive stars are not greatly underestimated. The formation of close massive BH–BH binaries requires that after the main sequence (4) VMSs above $500 M_{\odot}$ expand significantly (by more than a factor of 2), (5) their H-rich envelopes have a mass larger than $10\text{--}100 M_{\odot}$, (6) the evolution of such a binary involves a common envelope phase, and (7) the binary can survive the common envelope phase while the donor star is a very massive HG star. If conditions (4) through (7) are not met, then isolated binary evolution (i.e., field stellar populations) may produce only wide massive BH–BH binaries. We point out that even if these requirements are not met, there are several dynamical processes that could lead to efficient lowering of the coalescence time of wide massive BH–BH binaries both in dense stellar environments (cluster binary-single interactions) and in low-density field populations (Kozai mechanism in triple systems).

The resulting BH–BH merger rates depend sensitively on the amount of star forming mass with low metallicity at

redshifts $z < 2$ (the maximum distance at which a $100\text{--}100 M_{\odot}$ BH–BH binary will be detectable with the advanced LIGO/Virgo network). The amount of low metallicity star formation in the last Gyr may have been as high as $\sim 50\%$ of total star formation (Panter et al. 2008), and may have been even higher at the redshifts $z > 1$ that dominate our overall rates. Population synthesis models predict that 75% of the close massive BH–BH systems merge within 1 Gyr of formation. Based on simple estimates we find that realistic advanced LIGO/Virgo detection rates for these massive BH–BH systems are on the order of a few per year. However, the large uncertainties that burden our predictions allow for rates as high as hundreds of detections per year to as low as no detections at all.

BH–BH systems originating from isolated binaries of VMSs would likely have rather large mass ratios ($q \gtrsim 0.8$) and aligned spins. For a core collapse of a massive star that was spin-aligned with the orbit via tidal interactions with its companion, and that ejects no mass and has no linear momentum kick resulting from the collapse, our strong expectation is that the compact remnant would have a spin aligned with the orbit. Given our still-rudimentary understanding of core collapses there are of course situations in which this might not be accurate (e.g., oppositely directed neutrino jets on opposite sides of the proto-neutron star could impart spin angular momentum without imparting linear momentum), but at present such scenarios seem contrived. Regular ($M_{\text{zams}} < 150 M_{\odot}$) stars could not produce binaries with total mass in the $M_{\text{tot}} \gtrsim 100\text{--}200 M_{\odot}$ range. Therefore, detections of coalescences between massive, aligned, rapidly spinning BHs would uniquely identify systems originating from isolated binaries of VMSs. Such detections would indicate that the stellar IMF extends well beyond previously considered limits, and probably as high as $M_{\text{zams}} > 500 M_{\odot}$, and that massive progenitor binaries survive common envelope events even if the donors initiating these events are still in early evolutionary stages (i.e., on HG). This would also argue against models of VMSs that predict minimal expansion during post main-sequence evolution.

If observations show evidence for significant misalignment of BH spins, then either these systems received kicks via asymmetric neutrino emission or dynamical processes must have been involved in the formation of the merging BH–BH system. Moreover, Kalogera (2000) argued that significant spin–orbit misalignment is unlikely even with supernova kicks, unless dynamical effects are involved. This latter scenario would support the first set of published models of VMSs that show no (or very small) radial expansion (Yusof et al. 2013). Alternatively, mergers of intermediate-mass BHs could be a consequence of dynamical processes in globular clusters or involving globular cluster mergers (Fregeau et al. 2006; Amaro-Seoane & Santamaria 2009; Gair et al. 2011). Regardless, the detection of such systems would yield valuable information about dynamical encounters and/or the multiplicity of VMSs.

If instead we do not detect any massive BH–BH binaries with advanced LIGO/Virgo, any or all of the effects (1)–(7) discussed above may have contributed.

When mass is transferred from the secondary to the primary after the primary has evolved to become a BH, the binary may be visible as an ultra-luminous X-ray source (ULX), as the mass loss rate from the massive secondary can be very high. This stage is likely to be quite short, given that both companions are assumed to be massive and will have quite similar lifetimes. If 10% of all such binaries have a ULX stage lasting 1 million years—or, equivalently, all binaries have a

ULX stage lasting 100,000 yr—the space density of observable ULXs created through this channel will be equal to the merger rate times 10^5 yr. Since this is only one of several channels for creating ULXs, an observed ULX space density of a few $\times 10^{-2}$ Mpc^{-3} (Swartz et al. 2011) yields an upper limit on the massive binary merger rate of a few $\times 10^{-7}$ Mpc^{-3} yr^{-1} . This is a factor of several hundred higher than our very rough estimate of 10^{-9} Mpc^{-3} yr^{-1} , so it would be easy to hide the population of interest among the observed ULXs.

One possible constraint on the population of massive stars comes from rates of pair-instability supernovae. If an IMF slope of ~ -2.5 is extended to arbitrarily high masses, then $\sim 1\%$ of all stars having a ZAMS mass above $8 M_{\odot}$ will have a ZAMS mass above $200 M_{\odot}$. Hence, if a significant fraction of VMSs end their life in pair-instability supernovae, one might expect as many as 1% of all core-collapse supernovae to be pair-instability supernovae. Meanwhile, recent work by Nicholl et al. (2013) finds that this fraction is no more than 10^{-4} , and may be $<10^{-5}$, if the so-called “superluminous” supernovae are inconsistent with expectations of pair instability supernovae (Nicholl et al. 2013). If pair-instability supernovae only produce superluminous supernovae, these observations constrain either the number of massive stars exceeding $\sim 150 M_{\odot}$ or the mass range of stars that produce pair-instability supernovae. In such a scenario, if advanced LIGO/Virgo observes a large fraction of massive binary BH mergers, it would place constraints on the pair-instability mechanism and the mass range for which it occurs. Unfortunately, pair-instability supernovae seem to be able to produce a wide range of light curves (Kasen et al. 2011; Whalen et al. 2014) and until these light-curves can be better understood, it will be difficult to make any firm conclusions using superluminous supernova observations.

In conclusion, advanced LIGO/Virgo detectors are sensitive to the merger of massive BH binaries out to extraordinary distances ($z \sim 2$). We argue that the rate density of these mergers is such that event rates of a few per year, and perhaps as many as hundreds per year, are possible given current uncertainties in stellar evolutionary physics. The upper limits or detections expected from the coming generation of advanced ground-based GW instruments will provide unique insights into the evolution of VMSs.

The authors thank Mirek Giersz, Duncan Brown, and especially Vicky Kalogera for useful comments. K.B. and M.W. acknowledge support from Polish Science Foundation “Master2013” Subsidy, by Polish NCN grant SONATA BIS 2. K.B. also acknowledges NASA grant No. NNX09AV06A and NSF grant No. HRD 1242090 awarded to the Center for Gravitational Wave Astronomy, UTB. A.B. acknowledges support from NSF grant No. PHY-1208881 and NASA grant NNX12AN10G. D.E.H. acknowledges support from NSF CAREER grant PHY-1151836. I.M. was partly supported by STFC, including an ET R&D grant funded within the ASPERA-2 framework. M.C.M. acknowledges NASA grant NNX12AG29G, and a grant from the Simons Foundation (grant No. 230349). M.C.M. thanks the Department of Physics and Astronomy at Johns Hopkins University for hosting him during his sabbatical. The authors thank the Kavli Institute for Theoretical Physics (supported by the NSF grant No. PHY11-25915) for hospitality during the genesis of this project. The authors acknowledge the Texas Advanced Computing Center (TACC) at The University of Texas at Austin for providing computational resources used for this study.

REFERENCES

- Aasi, J., Abadie, J., Abbott, B. P., et al. 2013a, *PhRvD*, **88**, 062001
Aasi, J., Abadie, J., Abbott, B. P., et al. 2013b, *PhRvD*, **87**, 022002
Abadie, J., Abbott, B. P., Abbott, R., et al. 2010, *CQGra*, **27**, 173001
Abadie, J., Abbott, B. P., Abbott, R., et al. 2012, *PhRvD*, **85**, 102004
Abbott, B., Abbott, R., Adhikari, R., et al. 2009, *RPPh*, **72**, 076901
Accadia, T., Acernese, F., Alshourbagy, M., et al. 2012, *JInst*, **7**, 3012
Albrecht, S., Winn, J. N., Torres, G., et al. 2014, *ApJ*, **785**, 83
Amaro-Seoane, P., Gair, J. R., Freitag, M., et al. 2007, *CQGra*, **24**, 113
Amaro-Seoane, P., & Santamaria, L. 2009, *ApJ*, in press (arXiv:0910.0254)
Barkat, Z., Rakavy, G., & Sack, N. 1967, *PhRvL*, **18**, 379
Belczynski, K., Bulik, T., Fryer, C. L., et al. 2010a, *ApJ*, **714**, 1217
Belczynski, K., Bulik, T., Mandel, I., et al. 2013, *ApJ*, **764**, 96
Belczynski, K., Dominik, M., Bulik, T., et al. 2010b, *ApJL*, **715**, L138
Belczynski, K., Kalogera, V., Rasio, F. A., et al. 2008, *ApJS*, **174**, 223
Belczynski, K., Wiktorowicz, G., Fryer, C. L., Holz, D. E., & Kalogera, V. 2012, *ApJ*, **757**, 91
Blaes, O., Lee, M. H., & Socrates, A. 2002, *ApJ*, **578**, 775
Blondin, J. M., Mezzacappa, A., & DeMarino, C. 2003, *ApJ*, **584**, 971
Bond, J. R., Arnett, W. D., & Carr, B. J. 1984, *ApJ*, **280**, 825
Brown, D. A., Brink, J., Fang, H., et al. 2007, *PhRvL*, **99**, 201102
Buras, R., Rampp, M., Janka, H.-T., & Kifonidis, K. 2003, *PhRvL*, **90**, 241101
Cantiello, M., Langer, N., Brott, I., et al. 2009, *A&A*, **499**, 279
Carr, B. J., Bond, J. R., & Arnett, W. D. 1984, *ApJ*, **277**, 445
Chatzopoulos, E., Wheeler, J. C., & Couch, S. M. 2013, *ApJ*, **776**, 129
Claret, A. 2007, *A&A*, **467**, 1389
Colbert, E. J. M., & Mushotzky, R. F. 1999, *ApJ*, **519**, 89
Cooke, J., Sullivan, M., Gal-Yam, A., et al. 2012, *Natur*, **491**, 228
Crowther, P. A., Schnurr, O., Hirschi, R., et al. 2010, *MNRAS*, **408**, 731
Dewi, J. D. M., & Pols, O. R. 2003, *MNRAS*, **344**, 629
Dominik, M., Belczynski, K., Fryer, C., et al. 2012, *ApJ*, **759**, 52
Duchêne, G., & Kraus, A. 2013, *ARA&A*, **51**, 269
Duquennoy, A., & Mayor, M. 1991, *A&A*, **248**, 485
Figer, D. F. 2005, *Natur*, **434**, 192
Finn, L. S. 1996, *PhRvD*, **53**, 2878
Fregeau, J. M., Larson, S. L., Miller, M. C., O’Shaughnessy, R., & Rasio, F. A. 2006, *ApJL*, **646**, L135
Fryer, C. L., Belczynski, K., Wiktorowicz, G., et al. 2012, *ApJ*, **749**, 91
Fryer, C. L., & Heger, A. 2011, *AN*, **332**, 408
Fryer, C. L., & Kusenko, A. 2006, *ApJS*, **163**, 335
Fryer, C. L., Woosley, S. E., & Heger, A. 2001, *ApJ*, **550**, 372
Gair, J. R., Mandel, I., Miller, M. C., & Volonteri, M. 2011, *GReGr*, **43**, 485
Gal-Yam, A., Mazzali, P., Ofek, E. O., et al. 2009, *Natur*, **462**, 624
Glatzel, W., Fricke, K. J., & El Eid, M. F. 1985, *A&A*, **149**, 413
Glebbeek, E., Gaburov, E., de Mink, S. E., Pols, O. R., & Portegies Zwart, S. F. 2009, *A&A*, **497**, 255
Gräfener, G., Owocki, S. P., & Vink, J. S. 2012, *A&A*, **538**, A40
Gültekin, K., Miller, M. C., & Hamilton, D. P. 2006, *ApJ*, **640**, 156
Harry, G. M. the LIGO Scientific Collaboration. 2010, *CQGra*, **27**, 084006
Heggie, D. C. 1975, *MNRAS*, **173**, 729
Herant, M., Benz, W., & Colgate, S. 1992, *ApJ*, **395**, 642
Hinder, I., Buonanno, A., Boyle, M., Etienne, Z., et al. 2013, *CQGra*, **31**, 025012
Hinshaw, G., Larson, D., Komatsu, E., et al. 2013, *ApJS*, **208**, 19
Hjellming, M. S., & Webbink, R. F. 1987, *ApJ*, **318**, 794
Hogg, D. W. 1999, arXiv:astro-ph/9905116
Hurley, J. R., Pols, O. R., & Tout, C. A. 2000, *MNRAS*, **315**, 543
Ishii, M., Ueno, M., & Kato, M. 1999, *PASJ*, **51**, 417
Ivanova, N., Belczynski, K., Kalogera, V., Rasio, F. A., & Taam, R. E. 2003, *ApJ*, **592**, 475
Ivanova, N., Justham, S., Chen, X., et al. 2013, *A&ARv*, **21**, 59
Kalogera, V. 2000, *ApJ*, **541**, 042003
Kasen, D., Woosley, S. E., & Heger, A. 2011, *ApJ*, **734**, 102
Kato, M. 1985, *PASJ*, **37**, 311
Kiminki, D. C., & Kobulnicky, H. A. 2012, *ApJ*, **751**, 4
Kiminki, D. C., Kobulnicky, H. A., Ewing, I., et al. 2012, *ApJ*, **747**, 41
Kobulnicky, H. A., & Fryer, C. L. 2007, *ApJ*, **670**, 747
Kopparapu, R. K., Hanna, C., Kalogera, V., et al. 2008, *ApJ*, **675**, 1459
Kozai, Y. 1962, *AJ*, **67**, 591
Kroupa, P., Tout, C. A., & Gilmore, G. 1993, *MNRAS*, **262**, 545
Kusenko, A., & Segrè, G. 1996, *PhRvL*, **77**, 4872
Kusenko, A., & Segrè, G. 1997, *PhLB*, **396**, 197
Lang, C. C., Goss, W. M., & Rodríguez, L. F. 2001, *ApJL*, **551**, L143
Lidov, M. L. 1962, *P&SS*, **9**, 719
Lidov, M. L., & Ziglin, S. L. 1976, *CeMec*, **13**, 471

- LIGO Scientific Collaboration, & Virgo Collaboration., 2011, Advanced LIGO anticipated sensitivity curves, <https://dcc.ligo.org/cgi-bin/DocDB/ShowDocument?docid=2974>
- LIGO Scientific Collaboration, & Virgo Collaboration., 2013, LSC Algorithm Library software, <http://www.lsc-group.phys.uwm.edu/lal>
- LIGO Scientific Collaboration, et al. 2013, arXiv:1304.0670
- Loveridge, A. J., van der Sluys, M. V., & Kalogera, V. 2011, *ApJ*, **743**, 49
- MacFadyen, A. I., & Woosley, S. E. 1999, *ApJ*, **524**, 262
- Madau, P., & Rees, M. J. 2001, *ApJL*, **551**, L27
- Maeder, A. 1987, *A&A*, **173**, 247
- Mandel, I., Brown, D. A., Gair, J. R., & Miller, M. C. 2008, *ApJ*, **681**, 1431
- Massey, P. 2003, *ARA&A*, **41**, 15
- McKee, C. F., & Ostriker, E. C. 2007, *ARA&A*, **45**, 565
- Mennekens, N., & Vanbeveren, D. 2014, *A&A*, **564**, A134
- Miller, M. C., & Colbert, E. J. M. 2004, *IJMPD*, **13**, 1
- Miller, M. C., & Hamilton, D. P. 2002, *ApJ*, **576**, 894
- Nelemans, G., & Tout, C. A. 2005, *MNRAS*, **356**, 753
- Nicholl, M., Smartt, S. J., Jerkstrand, A., et al. 2013, *Natur*, **502**, 346
- Ofek, E. O., Zoglauer, A., Boggs, S. E., et al. 2014, *ApJ*, **781**, 42
- Panther, B., Jimenez, R., Heavens, A. F., & Charlot, S. 2008, *MNRAS*, **391**, 1117
- Paxton, B., Cantiello, M., Arras, P., et al. 2013, *ApJS*, **208**, 4
- Peters, P. C. 1964, *PhRv*, **136**, 1224
- Petrovic, J., Pols, O., & Langer, N. 2006, *A&A*, **450**, 219
- Podsiadlowski, P., Rappaport, S., & Han, Z. 2003, *MNRAS*, **341**, 385
- Punturo, M., Abernathy, M., Acernese, F., et al. 2010, *CQGra*, **27**, 084007
- Quinlan, G. D. 1996, *NewA*, **1**, 35
- Raymond, V., van der Sluys, M. V., Mandel, I., et al. 2010, *CQGra*, **27**, 114009
- Rodriguez, C. L., Mandel, I., & Gair, J. R. 2012, *PhRvD*, **85**, 062002
- Sana, H., de Koter, A., de Mink, S. E., et al. 2013a, *A&A*, **550**, A107
- Sana, H., de Mink, S. E., de Koter, A., et al. 2012, *Sci*, **337**, 444
- Sana, H., van Boeckel, T., Tramper, F., et al. 2013b, *MNRAS*, **432**, L26
- Schnittman, J. D. 2004, *PhRvD*, **70**, 124020
- Selman, F. J., & Melnick, J. 2013, *A&A*, **552**, A94
- Sepinsky, J. F., Willems, B., Kalogera, V., & Rasio, F. A. 2010, *ApJ*, **724**, 546
- Socrates, A., Blaes, O., Hungerford, A., & Fryer, C. L. 2005, *ApJ*, **632**, 531
- Swartz, D. A., Soria, R., Tennant, A. F., & Yukita, M. 2011, *ApJ*, **741**, 49
- Taracchini, A., Pan, Y., Buonanno, A., et al. 2012, *PhRvD*, **86**, 024011
- Tauris, T. M., & Dewi, J. D. M. 2001, *A&A*, **369**, 170
- Tauris, T. M., & Savonije, G. J. 1999, *A&A*, **350**, 928
- van der Sluys, M. V., Röver, C., Stroerer, A., et al. 2008, *ApJL*, **688**, L61
- Vink, J. S., de Koter, A., & Lamers, H. J. G. L. M. 2001, *A&A*, **369**, 574
- Virgo Collaboration. 2009, Advanced Virgo Baseline Design, Virgo Technical Report VIR-0027A-09, <https://tds.ego-gw.it/tds/file.php?callFile=VIR-0027A-09.pdf>
- Vitale, S., Lynch, R., Veitch, J., Raymond, V., & Sturani, R. 2014, *ApJ*, submitted (arXiv:1403.0129)
- Voss, R., & Tauris, T. M. 2003, *MNRAS*, **342**, 1169
- Webbink, R. F. 1984, *ApJ*, **277**, 355
- Weidner, C., Kroupa, P., & Pflamm-Altenburg, J. 2011, *MNRAS*, **412**, 979
- Wellstein, S., Langer, N., & Braun, H. 2001, *A&A*, **369**, 939
- Whalen, D. J., & Fryer, C. L. 2012, *ApJL*, **756**, L19
- Whalen, D. J., Smidt, J., Even, W., et al. 2014, *ApJ*, **781**, 106
- Wong, T.-W., Valsecchi, F., Ansari, A., et al. 2013, arXiv:1304.3756
- Woosley, S. E. 1993, *ApJ*, **405**, 273
- Woosley, S. E., Blinnikov, S., & Heger, A. 2007, *Natur*, **450**, 390
- Woosley, S. E., & Heger, A. 2012, *ApJ*, **752**, 32
- Xu, X.-J., & Li, X.-D. 2010, *ApJ*, **716**, 114
- Yusof, N., Hirschi, R., & Kassim, H. A. 2012, in IAU Symp. 279, Death of Massive Stars: Supernovae and Gamma-Ray Bursts, ed. P. Roming, N. Kawai, & E. Pian (Cambridge: Cambridge Univ. Press), 431
- Yusof, N., Hirschi, R., Meynet, G., et al. 2013, *MNRAS*, **433**, 1114